Manufacturing Rev. **12**, 8 (2025)

https://doi.org/10.1051/mfreview/2025006

Manufacturing Review
Available online at:
https://mfr.edp-open.org

ORIGINAL ARTICLE OPEN ACCESS

Mechanical behaviour and bio-corrosion performance of Zn-Cu-Mn based alloys for biomedical applications

Kenneth Kanayo Alaneme[1,2,*] and Michael Adediran[1]

[1] Materials Design and Structural Integrity Group, Department of Metallurgical and Materials Engineering, Federal University of Technology Akure, P.M.B. 704, Ondo State, Nigeria
[2] Centre for Nanoengineering and Advanced Materials, School of Mining, Metallurgy and Chemical Engineering, Faculty of Engineering & the Built Environment, University of Johannesburg, Johannesburg, South Africa

Received: 25 October 2024 / Accepted: 28 February 2025

Abstract. The mechanical behaviour and bio-corrosion properties of Zn-1.2Cu-xMn ($x = 0.2$, 0.4, and 0.6 wt%) alloys was investigated in this study. The alloy compositions were produced via liquid metallurgical processing and characterized using scanning electron microscopy (SEM), and X-ray diffractometry (XRD). The mechanical properties were evaluated using hardness, tensile properties, fracture toughness measurement while corrosion studies in Hank's solution was used to access the bio-corrosion behaviour. The results show that the tensile test of the studied Zn alloys increased in ultimate strength from 79.52 to 112.65 MPa, fracture toughness from 6.99 to 7.71 $MPam^{1/2}$ and hardness from 10.59 to 18.80 Hv, but with significant reduction in ductility from 5.21% to 3.63%. The improved mechanical properties were attributed to solid solution and second phase strengthening. The alloys presented appropriate in vitro degradation rates of 25–73 μm/year in Hank's solution. Based on the results demonstrated by the studied Zn-Cu-Mn alloys with suitable mechanical properties and ideal degradation behavior, it is projected as a promising candidate for cardiovascular stent applications.

Keywords: Zn based biometallic alloys / biodegradable materials / mechanical behaviour / stents / biomedical applications

1 Introduction

The implantation of biodegradable metals as temporary biomaterial implants (cardiovascular stents and orthopedic devices) to support healing and growth, has assisted in improving human lives, reducing challenges with permanent implants (second surgery) and facilitate a potential market for the biomedical industry [1,2]. In many biomedical applications, the safety and performance of materials are given top priority. So, factors such as significant mechanical properties, non-toxicity, biocompatibility and degradation rate drive their choice for medical devices [3–5]. In recent years, many studies have focused on biologically active metals such as magnesium (Mg) [6,7], iron (Fe) [8,9] and their alloys, and good clinical results have been obtained. For instance, the high strength, low density, and elastic modulus properties of Mg, predict their use in load bearing applications [10]. The higher strength of Mg bring about the development of orthopedic fixation devices like screws, pins and plates for medical purposes. Also, the close similarity attributes of Mg to human bones (41 GPa elastic modulus and 1.75 g/cm^3 density) promote the lessening of stress shielding difficulties and corroding of bones [11]. Fe, on the other hand, possess high strength, ductility and formability features, giving room for the fabrication of thinner stents and unique shapes (foils) [11,12]. However, the use of these materials are associated with complications such as speedy degradation of magnesium (rapid loss of integrity within 3 months after stent implantation, and complete disintegration within 4 months) and hydrogen gas development in vivo [13,14]. Similarly, iron-based alloys exhibit a slow degradation rate, resulting to tissue damage, with degradation products easily absorbed into the environment [15]. Zn is now appreciated and is receiving increasing attention as a substitute for magnesium and iron based alloys, reducing the disadvantages associated with the use of biodegradable metals for stenting applications.

Zinc is a very important element for the human body and is found mainly in the bone, skin, muscle, and liver [15,16]. The recommended daily allowance is between 2–3mg/day for children [17] and 6.5–15 mg/day for adults [18]. Zn many biological functions include aiding protein

* e-mail: kalanemek@yahoo.co.uk

metabolism, wound curing, and brain development [3,18,19]. Zinc functions in the prevention and treatment of many pathophysiological diseases, including cardiovascular, skeletal and neurological diseases as well as cancer [15]. For example, atherosclerosis is the most frequent cardiovascular disease, where the integrity of endothelial cells covering blood vessels disintegrate, undermining vascular functions and enhancing occlusive risk. So, zinc can protect the heart by protecting the endothelium [20]. To harness the therapeutic properties of zinc in various diseases, zinc can be modeled and integrated into a number of biomaterials, such as biodegradable stents and porous bone implants, giving support, nutrition and assist in the healing and growth of damaged blood vessels and the formation of new bone [21]. Their shortage can cause growth retardation, dermatitis, immune dysfunction, mental retardation, and delay wound curing [16–18]. According to the electrochemical series, zinc possesses an intermediate standard electrode potential of −0.762 V, relative to magnesium and iron [15,18]. Therefore, pure zinc displays intermediate corrosion rate when compared with Mg and Fe with non-toxic degradation products [21]. A report of the implantation of pure Zinc wire into the abdominal aorta of rats for a period of 6 months and 20 months by Bowel et al. [22] and Dvelich et al. [15] respectively, acknowledged their non-toxicity and excellent biocompatibility. Moreso, zinc and its alloys are easy to produce as a result of their minimum melting points temperatures [18].

The main purpose of designing a degradable metallic stent materials is to have the appropriate mechanical properties while maintaining the degradative attributes and biocompatibility. Although Zn has the potential for a degradable metallic stent materials due to its intermediate corrosion rate and excellent biocompatibility features, the intrinsic properties of pure zinc, namely strength (σUTS < 20 MPa) and ductility, appear to be low and unsatisfactory for design measures of cardiovascular stent materials [14,23]. To meet these needs, one of the best ways to enhance the performance of zinc for stent materials is alloying with trace elements, which are often considered [14,24]. Copper (Cu) and manganese (Mn) are thus selected.

Copper is an important component of the human body, and prior research has shown that it is not hazardous at daily dosage allowances of 10 mg/day for adults [25]. Its numerous health advantages include iron absorption, immune system support, and bone health maintenance [26–28]. Cu also functions as an antibacterial ion to avert infection during implantation [29]. Thus, the addition of Cu in zinc alloys would be of great benefits. Previous research has confirmed the viability of incorporating copper into zinc for clinical applications. Results from those researches showed that binary Zn-Cu alloys demonstrated improved mechanical properties, high biocompatibility, and reasonable corrosion rate. According to Niu et al. [26], the development and characterization of binary Zn-4Cu alloy for biomedical purposes brought about an average yield strength of 250 MPa and ultimate tensile strength of 270 MPa, good ductility of 51%, acceptable compatibility and uniform corrosion through extrusion method.

In addition, Zhang et al. [30] used a thermomechanical method to fabricate low alloyed Zn-2Cu-xLi alloys (x = 0, 0.004, 0.01, 0.07 wt%) for vascular stents. According to the results, Zn-2Cu-0.07Li has the best overall features of 321.8 MPa tensile strength, 362.3 MPa yield strength, 28% ductility and 89.5 μm/year degradation rate. Various researchers have also reported that the introduction of other trace elements (Al, Mg, Ca) to Zn-Cu binary alloys improves the material properties. However, their average strength needs to be further improved to obtain better material properties for effective stents performance [3,27,28].

In this research, the favorable solid solution interaction attributes of Mn encouraged its addition in Zn-1.2Cu alloys [29]. Manganese (Mn), like Cu, is a very tiny significant trace mineral contained in the human body at about 12 mg, and performs functions such as formation of connective tissue, sex hormones, and carbohydrates metabolism [31–33]. The recommended daily dose is 2 to 6 mg [31]. Although their micro alloying in Zn-Mn based alloys displayed enhanced material properties but their ternary addition in Zn alloys gave a better results [29,34,35]. Hence, the inclusion of Mn through micro alloying in Zn-Cu alloys is predicted to optimize the mechanical properties and corrosion resistance.

The present study investigates the mechanical behaviour and bio- corrosion properties of pure Zn and Zn-1.2Cu-xMn (x = 0.2, 0.4, and 0.6 wt%) alloys.

2 Material and methods

2.1 Alloys preparation

High purity Zn, Cu and Mn were purchased from a licensed distributor of chemical and industrial products in Nigeria, with pure zinc and experimental alloys Zn-1.2Cu-xMn (x = 0.2, 0.4 and 0.6 wt%) were designed from them using a crucible furnace. The alloy design began with charge calculations to determine the amount of alloying additions (copper and manganese) needed to produce three Zn-1.2Cu-Mn alloy compositions containing 0.2, 0.4, and 0.6 wt% Mn. Cu was thermally treated in a furnace at temperature of 1105 °C ± 20 °C until it was completely melted. The furnace temperature was then reduced to 700 °C, and after ensuring complete melting, the raw Zn metal was added. After cooling the Zn-Cu melt to a semi-solid state in the furnace, it was mixed for 5 min to achieve a homogenous mixture. Subsequently, Mn powder was then introduced and manually mixed for 10 min. The alloy slurry was subsequently heated to a temperature of 750 °C ± 10 °C and mechanically stirred for 6 minutes, after which it was poured into a cylindrical mold to facilitate air cooling. The cast ingots were heat treated via annealing at 300 °C for 3 h, then air cooled. The annealed ingots were machined into different test sizes, again annealed at 300 °C for 1 h and air cool to relieve the residual stresses in the samples as a result of the machining operation.

2.2 Microstructure characterization

2.2.1 Microstructural analysis

The microstructures of the annealed samples were examined using JSM 7600 F JEOL FEG-SEM. 240, 400, 600 grit and paper were used to ground the samples and polished (using 0.05 and 1 μm Al_2O_3 suspension) to a mirror like surfaces, etched using Keller's reagent (5 ml nitric acid, 3 ml hydrochloric acid, 2 ml hydrofluoric acid, 190 ml distilled water), swabbing for 10–20 s, rinsed with water, dried, and finally observed under a scanning electron microscope.

2.2.2 X-ray diffraction (XRD)

X-ray diffraction (XRD) was performed using a PANalytical X'Pert PRO (NIMS) to identify the samples crystalline phases present and their intensity. The scans were carried out repeatedly from 20 degree to 90 degree in 2-theta at a scan rate of 0.4 deg/min.

2.3 Mechanical testing

The mechanical properties of the annealed pure Zinc and Zn-1.2Cu-xMn ($x = 0.2$, 0.4 and 0.6 wt%) alloys were conducted using hardness test, tensile characterization and fracture evaluation.

Hardness measurements were obtained through a digital hardness tester, conforming to ASTM E18-16 [36] standards. The samples were subjected to a 100g load held for 15 seconds. A total of 6 indentations impact were taken on different samples and the values of their average recorded as the samples hardness.

Tensile characterization was observed using a universal testing machine (Hounsfield Tensiometer, type "W") in compliance with ASTM E8M-15a [37] protocols. The tests were observed using a strain rate of 0.00208/s on all tensile samples of 60mm gauge length and 6.5 mm diameter.

The fracture toughness evaluation of annealed pure Zn and Zn-Cu-Mn alloys were assessed through the circumferential notch tensile (CNT) test method, as described by Alaneme [38]. The test specimens with measured dimensions (60 mm gauge length, 6.5 mm notch diameter and 60° notch angle) were used for the test at strain rate of 1×10^{-3}/s on the universal testing machine (Hounsfield Tensiometer, type "W"). The fracture load (pf) of the specimens were determined using the specimen load-displacement curves. The fracture toughness were calculated using the relation below;

$$K_{IC} = \frac{pf}{D^{3/2\left(1.729\left(\frac{D}{d}\right)\right)-1.27)}} \tag{1}$$

where: K_{IC} isfracture toughness, pf is the fracture load, D is the specimen gauge diameter (mm), d is the specimen notched diameter (mm).

The plane strain values were assessed for the material and specimen configuration using the following relation as outlined by Alaneme [38].

$$\mathrm{D} \geq \left(\frac{K_{IC}}{\sigma_{\mathrm{y}}}\right)^2 \tag{2}$$

where K_{IC} is the fracture toughness (MPa $m^{1/2}$) and σ_y is the yield strength (MPa) of the specimens.

2.4 Invitro corrosion test

Electrochemical testing was performed on the specimens after polishing (with SiC paper up to 3000 grits), washing and drying. Electrochemical analysis was conducted in Hank's balanced salt solution (HBSS) at 37 °C. The tests involved three-electrodes: the sample was used as the working electrode, the platinum plate was used as the counter electrode, and the saturated calomel electrode (SCE) was used as the reference electrode. The open circuit potential (OCP) was stabilized for 60 min. Potential dynamic curves were generated by scanning the potential from −1.15 to −0.93 V at a scan rate of 0.16 mV/s. The corrosion current density (icorr) and corrosion potential (E_{corr}) were obtained using Tafel extrapolation method. According to ASTM-G102- 89 [39], corrosion rate can be evaluated using the equation below:

$$\mathrm{CR} = \mathrm{K}_1 \frac{i\mathrm{cor}}{\rho} \times \mathrm{EW} \tag{3}$$

$$\mathrm{EW} = \frac{1}{\sum\left(\frac{n_i f_i}{w_i}\right)} \tag{4}$$

where CR is given in mm/year, i_{corr} is the corrosion current density in μA/cm^2, EW is the equivalent weight of the alloy, K_1 is 3.27 $\times 10^{-3}$, mm g/μA cm year, ρ is the density in g/cm^3, f_i is the mass fraction of the ith element in the alloy, W_i is the atomic weight of the ith element in the alloy, and n_i is the valence of the ith element of the alloy.

3 Results and discussion

3.1 Microstructure

The microstructures of the annealed pure Zn and Zn alloys are presented in Figure 1. Heterogeneous grain size distribution in a nonaligned way were observed in annealed Zn alloys while the grains of annealed pure Zn were homogenous in nature in an orderly manner. The addition of Cu and Mn in Figures 1b–1d leads to the formation of ε($CuZn_4$) and $MnZn_{13}$ within the Zn matrix [29]. The spherical second phase was revealed as ε($CuZn_4$) phase according to SEM and XRD results. The addition of Mn enabled the dissolution of Mn in ε phase to replace part of Cu and reduces the grain size of the Zn matrix. It is apparent from Figures 1c–1d that an additional second phase identified as $MnZn_{13}$, with its volume fraction increased with Mn addition. Also, from Figures 1c–1d, ε($CuZn_4$) phase was brighter than $MnZn_{13}$ phase. The annealed pure Zn contained only one phase (ηZn) while the studied Zn alloys contained multiple phases (ηZn, ε($CuZn_4$) and $MnZn_{13}$).

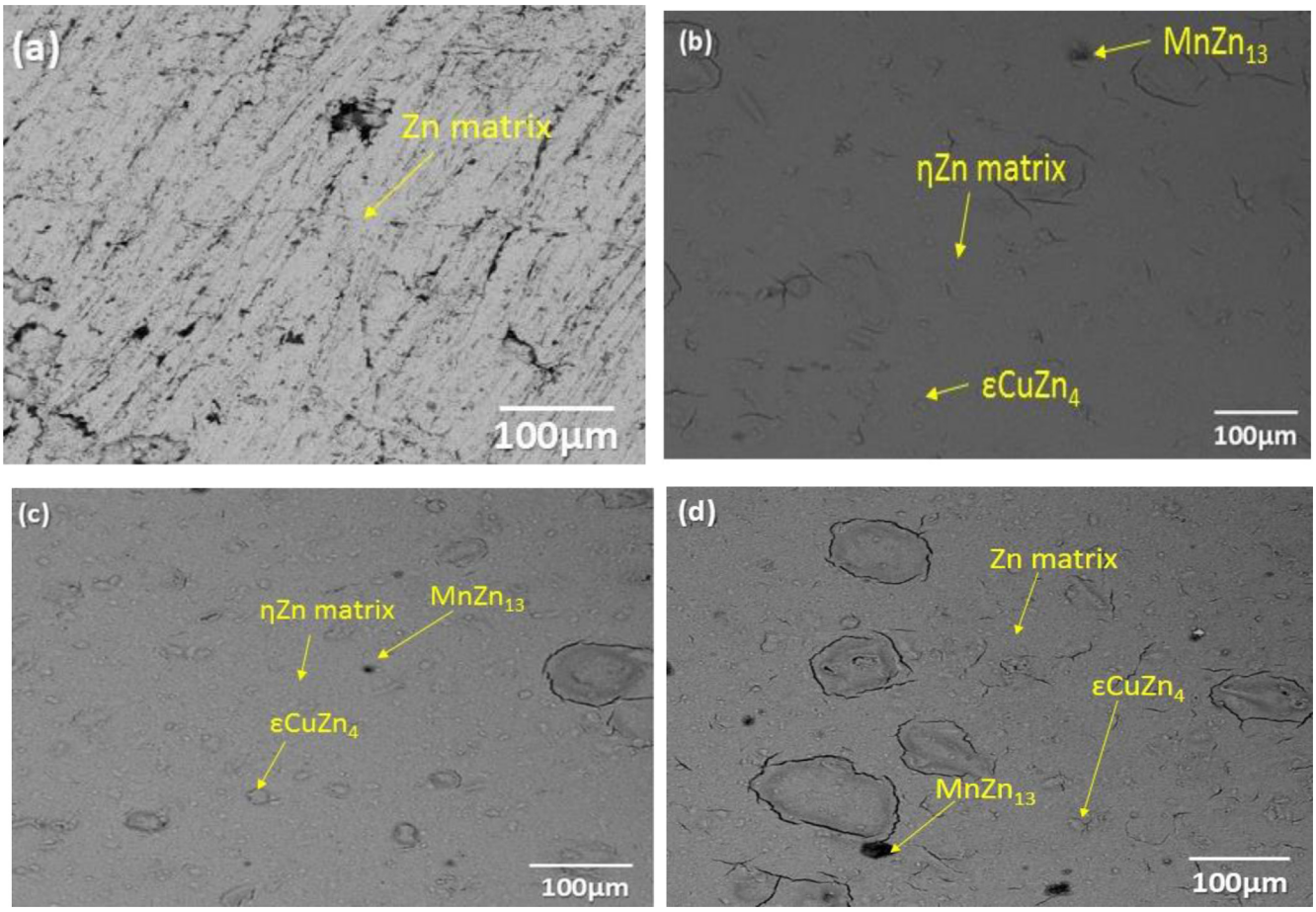

Fig. 1. SEM images showing the morphologies of annealed pure Zn and Zn alloys: (a) Zn(b) Z (b) Zn-1.2Cu-0.2Mn (c) Zn-1.2Cu-0.4Mn (d) Zn-1.2Cu-0.6Mn.

3.2 X-ray diffraction (XRD)

Figure 2 illustrates the XRD analysis of annealed pure Zn and Zn-1.2Cu-xMn alloys with various manganese contents. It is noticeable that ηZn matrix is the dominant phase present in all the study Zn alloys. The addition of 0.2, and 0.4 w% Mn displaced mainly of two phases (ηZn matrix and $\varepsilon CuZn_4$) while 0.6 wt% Mn consists of mainly three phases (ηZn matrix, $\varepsilon CuZn_4$ and $MnZn_{13}$).

3.3 Mechanical properties

The mechanical test results for annealed pure Zn and Zn alloys are presented in Figures 3–6. For the hardness test results (Fig. 3), the annealed pure Zn had the lowest average hardness of 10.59 Hv while the annealed Zn-1.2Cu-0.6Mn had the highest average hardness of 18.80 Hv. The average hardness for annealed Zn-1.2Cu-xMn alloys increased by 15, 50, 78% with increase in the Mn content of 0.2, 0.4 and 0.6 wt%, respectively. The main strengthening mechanism responsible for more hardness value of the annealed Zn alloys as compared to Zn is solid solution strengthening, where the lattice strains are induced by the solute atoms of Cu and Mn, in addition to the counteraction of the grain weakening effects of the dislocations [29,35,40].

The ultimate tensile strength results are presented in Figure 4. The strength of the annealed pure Zn sample is lower than their Zn alloy counterparts. As the Mn content increased from 0.2 to 0.6 wt%, the annealed Zn-Cu-Mn alloys experienced an appreciable 23, 33, 42% increase in mechanical strength which is in good agreement with the previous work [35]. This increase can be ascribed to two reasons. The major reason can be linked to the secondary phase precipitates formed [29]. The small particles (second phase) hindered dislocation movement. Increasing the Mn concentration in Zn-Cu-Mn alloys, larger amount of $MnZn_{13}$ is experienced, giving more dislocation barriers and improved strength. The second reason may be attributed to strengthening method through alloying of Zn with Cu and Mn known as solid solution strengthening [40], increasing the content of Mn resulted in a corresponding increase in strength, exhibiting a similar trend to hardness (Fig. 3).

Dissimilarly, the percentage elongation of the samples (Fig. 5) follow the reverse trend from that observed for hardness (Fig. 3) and ultimate tensile strength (Fig. 4). The annealed pure Zn had the highest percentage elongation while alloy with the highest Mn content had the least ductility. The percentage elongation of the studied Zn alloys decreased by 44, 28, 15%, as the concentration of Mn increases from 0.2 to 0.6 wt%,

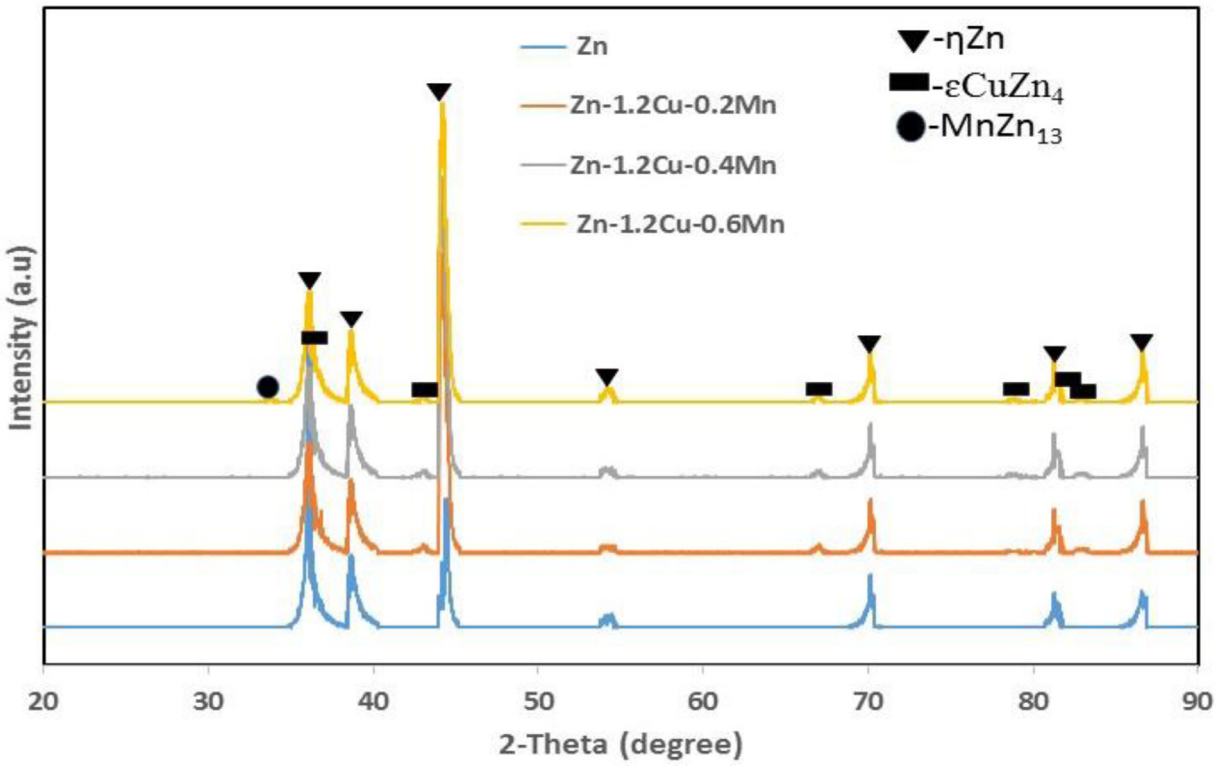

Fig. 2. XRD of the annealed pure Zn and Zn-based alloys produced.

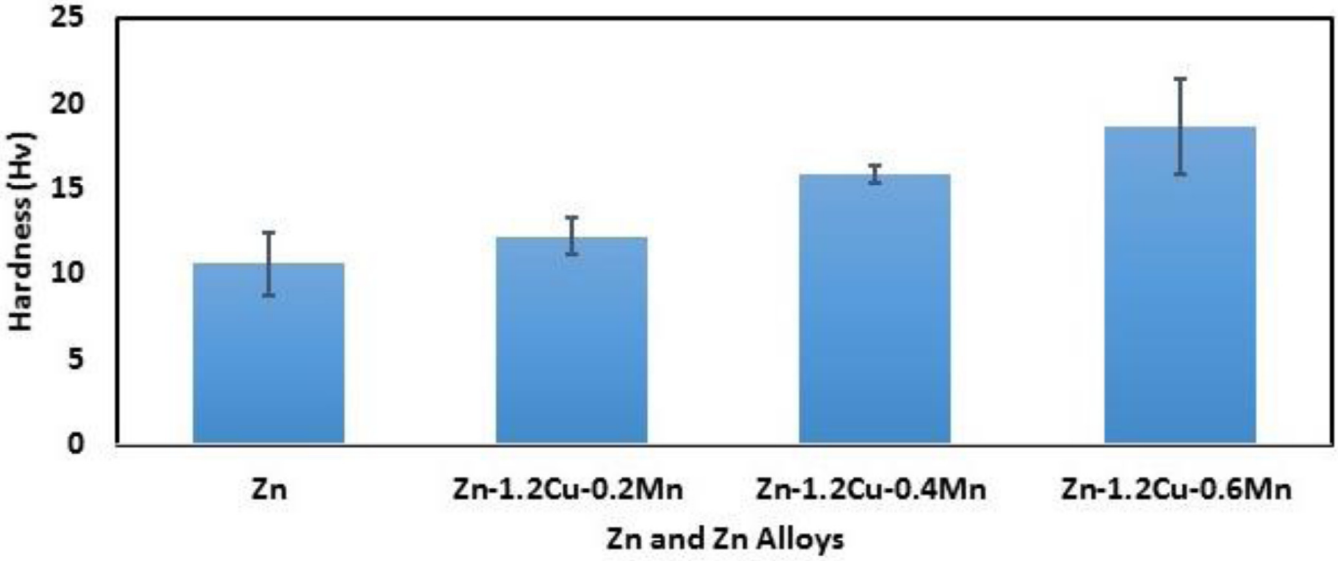

Fig. 3. Hardness values for the annealed pure Zn and Zn-based alloys.

respectively. The significant reduction in percentage elongation of the annealed Zn-Cu-xMn alloys compared to annealed Zn can be as a result of the presence of hard second phase [29]. The hard second phases dispersed in the ηZn matrix, serve as barriers to the movement of dislocation, resulting in stress concentrations pile up at the second phase and at certain stress level, initiate crack propagation. As the volume fraction of ηZn matrix reduces in the Zn-1.2Cu-xMn alloys, persistence crack path are formed easily with the higher hardness second phases, which decreases the percentage elongation of the studied alloys especially the Zn alloy with 0.6 wt% of Mn.

The fracture toughness results in Figure 6 show marginal increase in fracture toughness values as the Mn content increases. The pure Zn had the least fracture toughness value of 6.99 MPa $m^{1/2}$ while Zn-1.2Cu-0.6Mn

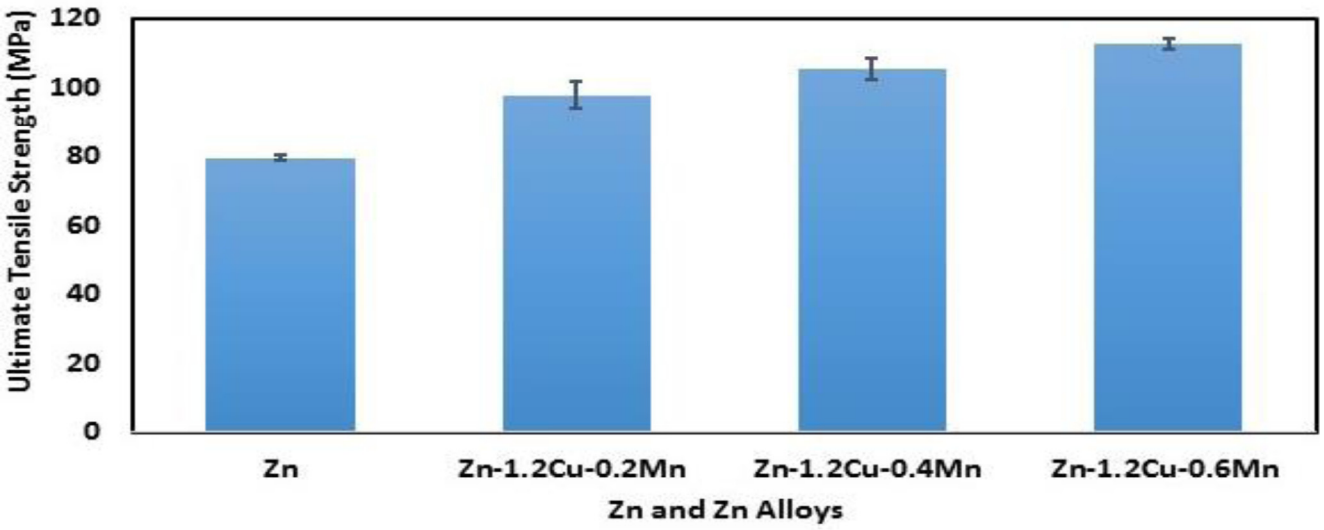

Fig. 4. Ultimate tensile strength for the annealed pure Zn and Zn-based alloys.

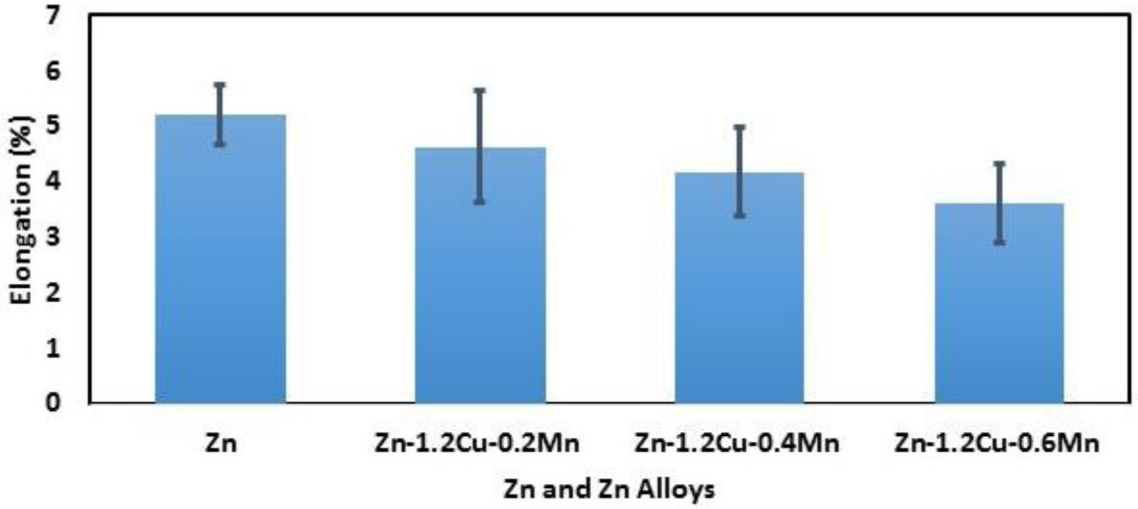

Fig. 5. Percentage elongation for the annealed pure Zn and Zn-based alloys.

alloy had the highest fracture toughness value of 7.71 MPa $m^{1/2}$, with slight increase of 7, 9, 10% of Mn content of 0.2, 0.4, 0.6 wt%, respectively. The reason why the studied Zn alloys are having relatively better crack propagation resistance to pure Zn is the formation of the second phases [3]. These hard second phases may increase the threshold stress intensity factor required for the commencement of crack growth in the alloys.

3.4 In vitro corrosion

Figures 7 and 8 showed the potentiodynamic polarization curves and degradation rates of annealed Zn and Zn-based alloys produced in Hank's solution respectively. Figure 7 shows that the alloys display similar polarization and passivation characteristics; however, Table 1 outlines the obtained results from the polarization curves using Tafel fitting. The annealed pure Zn displayed lower corrosion potential and higher polarization resistance of −1.0547 V and 3041Ω respectively, as compared with annealed Zn-1.2Cu-0.2Mn (–1.0588 V corrosion potential and 2253Ω polarization resistance), annealed Zn-1.2Cu-0.4Mn (–1.0558 V corrosion potential and 1706.3Ω polarization resistance), and annealed Zn-1.2Cu-0.6Mn (–1.0557 V corrosion potential and 1033.8Ω polarization resistance). The reason for this, is as a result of the presence of the second phases (as the Mn content increases, the volume fraction of second phase also increases) which increases the degradation of developed annealed Zn alloys through micro galvanic corrosion [29]. The annealed pure Zn displayed the lowest corrosion rate of 25.173 μm/year as presented in Figure 8. As the Mn content rises, the corrosion rate of the annealed Zn alloys also rises, with Zn-1.2Cu-0.2Mn, Zn-1.2Cu-0.4Mn, and Zn-1.2Cu-0.6Mn having corrosion rates of 35.938 μm/year, 44.22 μm/year and 72.774 μm/year respectively.

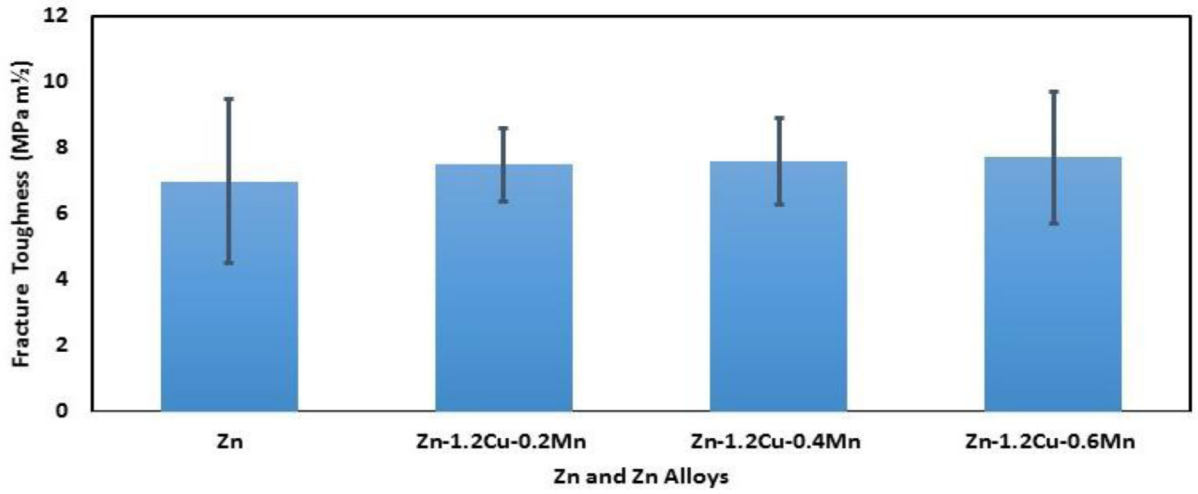

Fig. 6. Fracture toughness for the annealed pure Zn and Zn-based alloys.

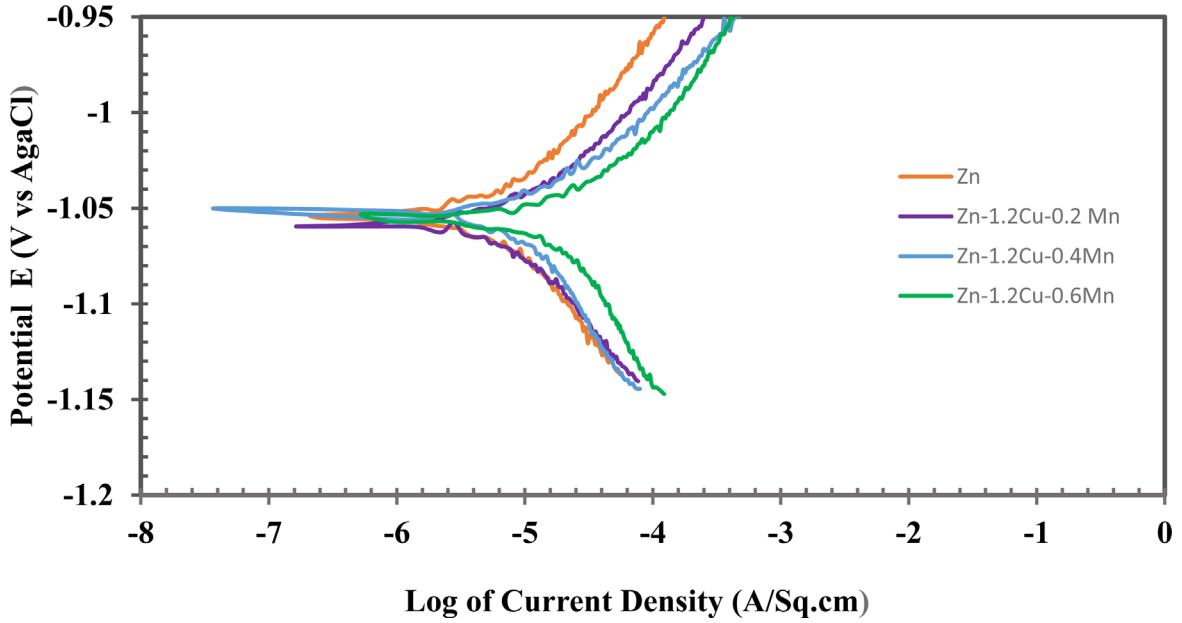

Fig. 7. Potentiodynamic polarization curves for the annealed Zn and Zn-based alloys in Hank's solution.

4 Conclusion

A new pure Zn and Zn-1.2Cu-xMn ($x = 0.2$, 0.4, 0.6 wt.%) alloys were synthesized and evaluated for biodegradable biomedical device applications. The preparation of the materials were by metal casting method and homogenization treatment. The effects of alloys composition on hardness, tensile properties, fracture toughness, and corrosion resistance in Hank's solution were investigated, which resulted to the following conclusions:

- The production of pure Zn and Zn-Cu-Mn alloys using double stir casting method were easy to cast, cost effective, prevented segregation/agglomeration of the reinforcement particles within the Zn matrix, lower porosity levels and better wettability due to good interphase bonding between the matrix/reinforcement particles. Annealing the samples before and after machining operations relieved the residue stresses in the samples.
- SEM analysis confirm the presence of mainly ηZn phase for annealed pure Zn and multiple phase aggregates such as ηZn matrix and stiff second phase ($\varepsilon CuZn_4$ and $MnZn_{13}$) for the Zn-1.2Cu-xMn ($x = 0.2$, 0.4, 0.6 wt.%) alloys.
- The XRD analysis showed that ηZn matrix is the dominant phase present in annealed pure Zn and in all the study Zn alloys. The addition of 0.2, and 0.4 w% Mn displayed mainly of two phases (ηZn matrix and $\varepsilon CuZn_4$) while 0.6 wt% Mn consists of mainly three phases (ηZn matrix, $\varepsilon CuZn_4$ and $MnZn_{13}$).

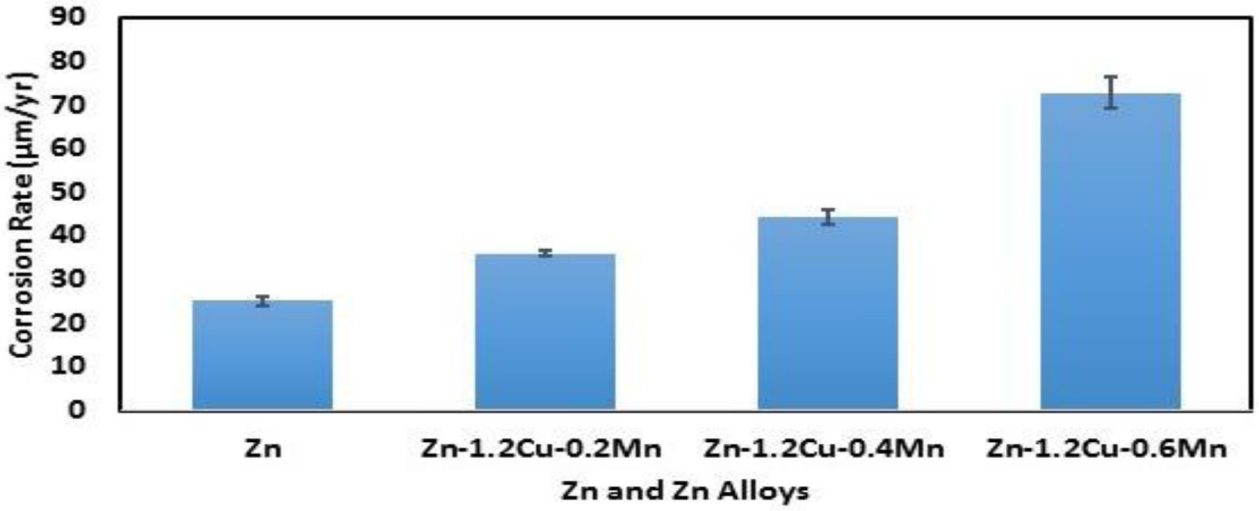

Fig. 8. Corrosion rates of annealed pure Zn and Zn-based alloys produced.

Table 1. Corrosion rates of annealed pure Zn and Zn-based alloys produced in Hank's solution obtained from fitting results of polarization curves.

Samples	Electrochemical	test		
	E_{corr} (V)	j_{corr} (A/cm^2)	Corrosion rate (μm/year)	Polarization resistance (Ω)
A(Zn)	–1.0547	0.0000021659	25.173	3041
B(Zn-1.2Cu-0.2Mn)	–1.0588	0.0000030927	35.938	2253
C(Zn-1.2Cu-0.4Mn)	–1.0558	0.0000038059	44.22	1706.3
D(Zn-1.2Cu- 0.6Mn)	–1.0557	0.0000062625	72.774	1033.8

– The studied Zn alloys exhibited increase in ultimate strength to 112.65 MPa, fracture toughness to 7.71 MPam$^{1/2}$ and hardness to 18.80 Hv, but with significant reduction in ductility to 3.63% with increase in Mn content to 0.6 wt.%.
– The Zn-1.2Cu-xMn alloys displayed suitable corrosion rates of 25–73 μm/year in Hank's solution.

Funding

The authors wish to appreciate the support of their institutions, and the National Research Foundation (NRF), South Africa through the Grant No: 138062, administered by The University of Johannesburg, South Africa.

Conflicts of interest

The authors declare no conflicts of interest.

Data availability statement

The research data would be made available on request.

Author contribution statement

Kenneth Kanayo Alaneme (KKA) conceptualized and designed the research, verified the analytical methods and analysis, supervised the research, developed, revised and finalized the manuscript with MA, and facilitated funding for the research. Michael Adediran (MA) engaged in the experimental investigation and data analysis, contributed to the manuscript development, revision and finalization.

References

1. D. Vojtěch, J. Kubásek, J. Šerák, P. Novák, Mechanical and corrosion properties of newly developed biodegradable Zn-based alloys for bone fixation, Acta Biomater. **7** (2011) 3515–3522
2. P.K. Bowen, E.R. Shearier, S. Zhao, R.J. Guillory, F. Zhao, J. Goldman, J.W. Drelich, Biodegradable metals for cardiovascular stents: from clinical concerns to recent Zn-alloys, Adv. Healthc. Mater. **5** (2016) 1121–1140
3. K.K. Alaneme, J.C. Edwin-Ezeh, Mechanical characteristics and biocorrosionbehaviour of AS-CAST Zn-3Cu-Al alloys for cardiovascular bioabsorbable devices, Mater. Today: Proc. **62** (2022) S49–S56

4. D.G. Rizik, J.B. Hermiller, D.J. Kereiakes, Bioresorbable vascular scaffolds for the treatment of coronary artery disease: clinical outcomes from randomized controlled trials, Catheter. Cardiovasc. Interv. **88** (2016) 21–30
5. H.M. García-García, S. Vaina, K. Tsuchida, P.W. Serruys, Drug-eluting stents, Arch. Cardiol. Mex. **76** (2006) 297–319
6. M.I. Rahim, S. Ullah, P.P. Mueller, Advances and challenges of biodegradable implant materials with a focus on magnesium-alloys and bacterial infections, Metals **8** (2018) 1–14
7. J. Wang, J. Xu, B. Song, D.H. Chow, P. Shu-Hang Yung, L. Qin, Magnesium (Mg) based interference screws developed for promoting tendon graft incorporation in bone tunnel in rabbits, Acta Biomater. **63** (2017) 393–410
8. E. Mostaed, M. Sikora-Jasinska, A. Mostaed, S. Loffredo, A.G. Demir, B. Previtali, D. Mantovani, R. Beanland, M. Vedani, Novel Zn-based alloys for biodegradable stent applications: design, development and in vitro degradation, J. Mech. Behav. Biomed. Mater. **60** (2016) 581–602
9. B. Liu, Y.F. Zheng, Effects of alloying elements (Mn, Co, Al, W, Sn, B, C and S) on biodegradability and in vitro biocompatibility of pure iron, Acta Biomater. **7** (2011) 1407–1420
10. H. Gong, K. Wang, R. Strich, J.G. Zhou, In vitro biodegradation behavior, mechanical properties, and cytotoxicity of biodegradable Zn-Mg alloy, J. Biomed. Master. Res. B **103** (2015) 1632–1640
11. D. Zindani, K. Kumar, J.P. Davim, Metallic biomaterials—a review, J. Mech. Behav. Biomed. Mater. (2019) 84–99
12. R. Yue, H. Huang, G.Z. Ke, H. Zhang, J. Pei, G.H. Xue, G.Y. Yuan, Microstructure, mechanical properties and in vitro degradation behavior of novel Zn-Cu-Fe alloys, Mater. Charact. **134** (2017) 114–122
13. Z. Zhen, X. Liu, T. Huang, T. Xi, Y. Zheng, Hemolysis and cytotoxicity mechanisms of biodegradable magnesium and its alloys, Mater. Sci. Eng. C Mater. Biol. Appl. **46** (2015) 202–206
14. R. Yue, J. Niu, Y. Li, G. Ke, H. Huang, J. Pei, W. Ding, G. Yuan, In vitro cytocompatibility, hemocompatibility and antibacterial properties of biodegradable Zn-Cu-Fe alloys for cardiovascular stents applications, Mater. Sci. Eng. C **113** (2020) 111007
15. A.J. Drelich, S. Zhao, R.J. Guillory 2nd, J.W. Drelich, J. Goldman, Long-term surveillance of zinc implant in murine artery: surprisingly steady biocorrosion rate, Acta Biomater. **58** (2017) 539–549
16. P.H. Lin, M. Sermersheim, H. Li, P.H.U. Lee, S.M. Steinberg, J. Ma, Zinc in wound healing modulation, J. Nutr. **10** (2017) 16
17. C.P. Larson, S.K. Roy, A.I. Khan, A.S. Rahman, F. Qadri, Zinc treatment to under-five children: applications to improve child survival and reduce burden of disease, J. Health Popul Nutr. **26** (2008) 356–365
18. G.K. Levy, J. Goldman, E. Aghion, The prospects of zinc as a structural material for biodegradable implants—a review paper, Metals **7** (2017) 402
19. H. Kabir, K. Munir, C. Wen, Y. Li, Recent research and progress of biodegradable zinc alloys and composites for biomedical applications: biomechanical and biocorrosion perspectives, Bioact. Mater. **6** (2021) 836–879
20. T. Shen, Q. Zhao, Y. Luo, T. Wang, Investigating the role of zinc in atherosclerosis: a review, Biomolecules **12** (2022) 1358
21. Y. Su, I. Cockerill, Y. Wang, Y.X. Qin, L. Chang, Y. Zheng, D. Zhu, Zinc-based biomaterials for regeneration and therapy, Trends Biotechnol. **37** (2019) 428–444
22. P.K. Bowen, J. Drelich, J. Goldman, Zinc exhibits ideal physiological corrosion behavior for bioabsorbable stents, Adv. Mater. **25** (2013) 2577–2582
23. Y. Su, I. Cockerill, Y.D. Wang, Y.X. Qin, L.Q. Chang, Y.F. Zheng, D.H. Zhu, Zinc-based biomaterials for regeneration and therapy, Trends. Biotechnol. **37** (2019) 428–441
24. H. Li, H. Yang, Y. Zheng, F. Zhou, K. Qiu, X. Wang, Design and characterizations of novel biodegradable ternary Zn-based alloys with IIA nutrient alloying elements Mg, Ca and Sr, Mater Des. **83** (2015) 95–102
25. Institute of Medicine (US) Panel on Micronutrients. Dietary reference intakes for vitamin A, vitamin K, arsenic, boron, chromium, copper, iodine, iron, manganese, molybdenum, nickel, silicon, vanadium, and zinc. Washington (DC): National Academics Press (US); 2001. **7**, Copper. Available from: https://www.ncbi.nlm.nih.gov/books/NBK222312/#ddd00333
26. J. Niu, Z. Tang, H. Huang, J. Pei, H. Zhang, G. Yuan, W. Ding, Research on a Zn-Cu alloy as a biodegradable material for potential vascular stents application, Mater. Sci. Eng. C Mater. Biol. Appl. **69** (2016) 407–413
27. N. Yang, N. Sivamuni, N. Balasubramani, J. Venezuela, S. Almathami, C. Wen, M. Dargusch, The influence of Ca and Cu additions on the microstructure, mechanical and degradation properties of Zn-Ca-Cu alloys for absorbable wound closure device applications, Bioact. Mater. **6** (2021) 1436–1451
28. Z. Tang, H. Huang, J. Niu, L. Zhang, H. Zhang, J. Pei, J. Tan, G. Yuan, Design and characterizations of novel biodegradable Zn-Cu-Mg alloys for potential biodegradable implants, Mater. Des. **117** (2017) 84–94
29. J. Jiang, Y. Qian, H. Huang, J. Niu, G. Yuan. Biodegradable Zn-Cu-Mn alloy with suitable mechanical performance and in vitro degradation behavior as a promising candidate for vascular stents, Biomater Adv. **133** (2022) 112652.
30. X. Zhang, J. Niu, K. W-K.Yeung, H. Huang, Z. Gao, C. Chen, Q. Guan, G. Zhang, L. Zhang, G. Xue, G. Yuan, Developing Zn-2Cu-xLi ($x < 0.1$ wt %) alloys with suitable mechanical properties, degradation behaviors and cytocompatibility for vascular stents, Acta Biomater. (2024)
31. M. Rondanelli, M.A. Faliva, G. Peroni, V. Infantino, C. Gasparri, G. Iannello, S. Perna, A. Riva, G. Petrangolini, A. Tartara, Essentiality of manganese for bone health: an overview and update, Nat. Prod. Commun. **16** (2021) 1934578×2110166
32. R.G. Lucchini, M. Aschner, Y. Kim, M. Šarić, Manganese. Handbook on the Toxicology of Metals (Fourth Edition) Academic Press, (2015), pp. 975–1011
33. P. Chen, J. Bornhorst, M. Aschner, Manganese metabolism in humans, Front. Biosci. (landmark edition) **23** (2018) 1655–1679
34. Z.Z. Shi, J. Yu, X.-F. Liu, Micro alloyed Zn-Mn alloys: from extremely brittle to extraordinarily ductile at room temperature, Mater. Des. **144** (2018) 343–352
35. Z.Z. Shi, J. Yu, X.F. Liu, L.N. Wang, Fabrication and characterization of novel biodegradable Zn-Mn-Cu alloys, J. Mater. Sci. Technol. **34** (2018) 1008–1015

36. ASTM E18-16: Standard Test Method for Rockwell Hardness of Metallic Materials, ASTM International, West Conshohocken, PA 2016, www.astm.org
37. ASTM E8M-15a: Standard Test Method for Tension testing of Metallic Materials, ASTM International, West Conshohocken, PA, 2015, www.astm.org
38. K.K. Alaneme, Fracture toughness (K1C) evaluation for dual phase low alloy steels using circumferential notched tensile (CNT) specimens, Mat. Res. **14** (2011) 155–160
39. ASTM-G102-89: Standard practice for calculation for corrosion rates and related information from electrochemical measurements. In: Annual Book of ASTM Standards. Philadelphia, PA, USA: American Society for Testing and Materials. 2010
40. E. Mostaed, M. Sikora-Jasinska, J.W. Drelich, M. Vedani, Zinc-based alloys for degradable vascular stent applications, Acta Biomater. **71** (2018) 1–23

Cite this article as: Kenneth Kanayo Alaneme, Michael Adediran, Mechanical behaviour and bio-corrosion performance of Zn-Cu-Mn based alloys for biomedical applications, Manufacturing Rev. **12**, 8 (2025), https://doi.org/10.1051/mfreview/2025006